

Computer solutions of Maxwell's equations in homogeneous media

O. Pironneau^{*,†}

University of Paris VI and IUF, France

SUMMARY

This document is the material support for a talk given for JSIAM on the current methods for the computation of radar cross sections. The talk covers more than just computations of RCS and extends to any problem which involves the numerical solution of Maxwell's equations in homogeneous media. The talk is based on a review of the most recent papers in leading journals and on the author's experience. Copyright © 2003 John Wiley & Sons, Ltd.

KEY WORDS: inverse scattering problem; Maxwell's equations; radar cross sections

1. INVERSE SCATTERING PROBLEM

A precise definition of the radar cross section (RCS) of an object in a sector of vision Θ is irrelevant for what we wish to do here; it is complex and it can be found in books like Skolnik [1]. We only need to know that it has the dimension of a surface and is of the following form:

$$\text{RCS} \approx \frac{1}{T|E_\infty|^2} \int_0^T \int_{S \cap \Theta} |x|^2 |E|^2 \, d\theta \, d\varphi \, dt$$

where S is a sphere far from the object which reflects the incident electromagnetic signal $E(x, t)$, where T is the duration of the signal, θ, φ the spherical angles which define a point x on the sphere, $|E_\infty|$ the mean electromagnetic intensity of the incident signal and Θ the solid angle which specifies the direction of interest for the reflected signal (could be the whole space or a cone in the direction of the listener) (Figure 1).

For detection of airplanes and missiles of course one needs to know what the scattered (i.e. reflected) signal is when the object is lit by a radar signal. These radar signals are usually made of a long pulse containing a somewhat monochromatic wave. The frequency of the waves

^{*}Correspondence to: O. Pironneau, Université Pierre et Marie Curie, Laboratoire Jacques-Louis Lions, 4 Place Jussieu, 75252 Paris Cedex 05, France.

[†]E-mail: pironneau@anu.jussieu.fr

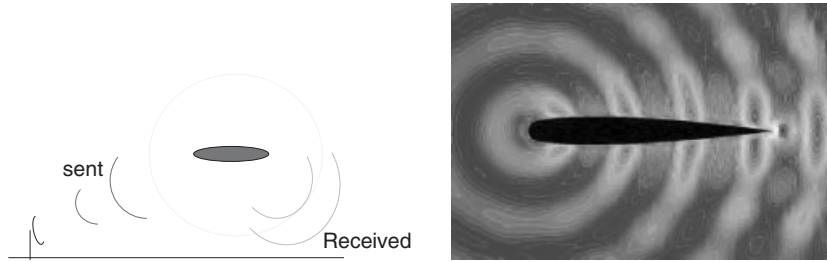


Figure 1. Left: the schematics of RCD. Right: a computation around a NACA0012 (courtesy of Remaki [2]).

varies widely, there is a race towards high frequencies and there is also much classified research for obvious reasons. There exist advanced coatings which are electromagnetically absorbing materials but we will not touch this difficult and also classified subject. So we are dealing with an incident wave coming from infinity, a perfectly reflecting object (usually a perfect conductor) and an infinite medium around it, typically air because, in the case of flying objects, the ground is far away and can be neglected except for low altitude flights.

2. MAXWELL'S EQUATIONS

An electromagnetic wave is characterized by an electric field $E(x, t)$ and a magnetic field $H(x, t)$. Then in a medium with electromagnetic constants ε, μ the equations read

$$\varepsilon \partial_t E - \nabla \times H = J$$

$$\mu \partial_t H + \nabla \times E = 0$$

$$\nabla \cdot (\mu H) = \rho$$

$$\nabla \cdot (\varepsilon E) = 0$$

where J is the current inside an object \dot{S} with surface S and ρ is the charge density in \dot{S} . These equations have to be integrated in $\mathcal{R}^3 \times (0, T)$ with different values for μ, ε in air and in the object, but to have a unique solution one must prescribe the behaviour of the solution at infinity, the so called Silver–Muller condition:

$$\lim_{|x| \rightarrow \infty} |x| \left(E - \frac{H \times n}{\sqrt{\varepsilon \mu}} \right) \times n = 0$$

For perfect conductors one may integrate the equations in $(\mathcal{R}^3 \setminus \dot{S}) \times (0, T)$ only and add boundary conditions on S such as (Figure 2)

$$E \times n = 0 \quad H \cdot n = 0 \quad \text{on } S$$

The first obvious difficulty is that there are more equations than there are variables: the system is over determined. In particular if the divergence equations are satisfied at time zero, then

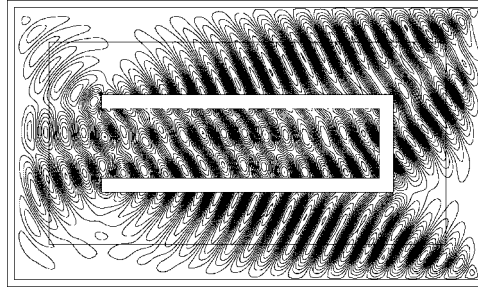


Figure 2. The open-box test case is difficult because there are closed rays and so the convergence to a periodic solution in time is at best polynomial. This result is from Morgan *et al.* [3].

they are also satisfied at later times. The next problem is the decay in time to zero for a compact initial data:

Proposition 1

The solution to Maxwell’s equations with the boundary conditions above and initial conditions on E and H exists and is unique for given $(E, H)|_{t=0}$ with compact support. It decays exponentially in time if there are no closed rays and at best polynomially otherwise.

2.1. Inductions

For notational and algorithmic reasons it is convenient to introduce the electric and magnetic inductions

$$D = \epsilon E \quad B = \mu H$$

Remark 1

Note that

$$\nabla \cdot J = 0 \quad \epsilon, \mu \text{ constant} \Rightarrow \nabla \cdot \mu H = \rho \quad \nabla \cdot \epsilon E = 0$$

3. SPECIAL CASES

3.1. TM and TE modes

Transverse magnetic and transverse electric solutions are by definition of the form

$$H = \begin{pmatrix} H_x \\ H_y \\ 0 \end{pmatrix} \quad E = \begin{pmatrix} 0 \\ 0 \\ E_z \end{pmatrix} \quad \leftarrow \text{TM TE} \rightarrow \quad E = \begin{pmatrix} E_x \\ E_y \\ 0 \end{pmatrix} \quad H = \begin{pmatrix} 0 \\ 0 \\ H_z \end{pmatrix}$$

If the initial condition and boundary conditions are in one of the above form and if the geometry is cylindrical then such solutions are possible. They are essentially two dimensional as seen by elimination of one of the variable.

3.2. Elimination of E (or H) in TE mode

$$\mu \partial_n H + \nabla \times \left(\frac{1}{\varepsilon} \nabla \times H \right) = 0$$

3.3. Monochromatic waves

Furthermore special solutions of the form $H_z(x, t) = e^{i\omega t} u(x)$ are possible and u is then solution of a Helmholtz equation:

$$\kappa^2 u + \Delta u = 0, \quad \kappa = \omega^2 \mu \varepsilon$$

3.3.1. *In a half space.* When S is the plane $x \cdot n \geq 0$ and with a monochromatic incident wave $u^i = e^{ik \cdot x}$, $|k| = \kappa$ there is an analytical solution

$$u = e^{ik \cdot x} - e^{i\bar{k} \cdot x} \quad \bar{k} = k - 2(n \cdot k)n$$

These are interpreted as Descartes' geometrical construction for the reflected signal because it is symmetrical to the incident wave with respect to the normal of the plane.

3.3.2. *Cylinder.* When S is a cylinder and the incident wave has TM or TE polarization then there is an analytical solution to the Maxwell equations in terms of special functions; define P_n as the Legendre function, J_n as the Bessel function of the first kind and H_n as the Hankel function:

$$u^s = - \sum_{n=0}^{\infty} i^n (2n+1) \frac{j_n(kR)}{h_n(kR)} h_n(k|x|) P_n \left(\frac{k \cdot d}{|k||d|} \right)$$

3.3.3. *Sphere.* When S is a sphere there is also a semi-analytical solution. Furthermore whatever the boundary conditions a Fourier expansion of solution is known outside the cylinder/sphere.

4. GEOMETRICAL AND PHYSICAL OPTICS

At high frequencies it is reasonable to assume that the incident wave 'sees' S almost as if it was its tangent plane. With such an approximation one may assume that Descartes' law of reflections are true (cf. Figure 4) and then construct the reflected signal by a purely geometrical construction with ray going from the source in all directions onto the object and reflected by a symmetry with respect to the normal of S . This explains why stealth airplanes tend to privilege flat surfaces (Figure 3).

One may go one step further in precision with *physical optics*.

We will see later that the solution of Helmholtz equation satisfies

$$u(x) = u^i(x) - \int_{\Gamma} \left[\frac{\partial u}{\partial n}(y) \right] \frac{e^{i\kappa|x-y|}}{4\pi|x-y|} d\gamma(y)$$

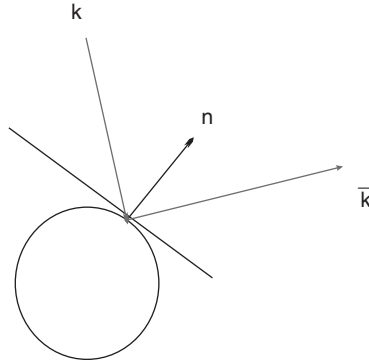


Figure 3. Geometrical optics.

If, in this formula we apply the approximation of geometrical optics to $\partial_n u$ then its jump across S is

$$\left[\frac{\partial u}{\partial n} \right] \approx 2 \frac{\partial e^{ik \cdot y}}{\partial n} = 2ik \cdot n e^{ik \cdot y}$$

and so

$$u(x) = u^i(x) - \int_{\Gamma} ik \cdot n \frac{e^{i(k \cdot y + \kappa|x-y|)}}{2\pi|x-y|} d\gamma(y)$$

This is/was the best method to compute the RCS until computing power allowed the full solution of Helmholtz equation and now the full time dependent Maxwell system.

5. TRUNCATION OF THE DOMAIN

5.1. Matching with an exact condition

Because the Fourier series of the general solution of Maxwell's equations is known outside a sphere, it is possible to match the computed solution inside a sphere and its first derivative with its outer expansion. This gives a non-local operator which is complex in general (see Reference [4]) but manageable for

$$k^2 u + \Delta u = 0 \quad \text{in } R^3 \setminus \dot{S} \quad u|_S = \lambda$$

This leads to the following numerical method: let the Dirichlet to Neumann operator be $\mathcal{M}(\lambda) = -\partial u / \partial n|_S$ then solve

$$k^2 u + \Delta u = 0 \quad \text{in } \dot{S} \setminus \Omega \quad u|_{\Gamma} = u_{\Gamma}, \quad \mathcal{M}(u) + \frac{\partial u}{\partial n} \Big|_S = 0$$

5.2. Transparent conditions

An outgoing monochromatic wave satisfies

$$\frac{\partial u}{\partial n} - i\kappa u = 0$$

therefore this relation can be used in conjunction with Helmholtz equation.

More precise conditions have been proposed such as the following second order condition:

$$-\frac{1}{2} \frac{\partial^2 u}{\partial s^2} + i\kappa \frac{\partial u}{\partial n} - k^2 u = 0$$

on the boundary of a square approximating infinity, together with jump conditions at the corner of the square:

$$ik\gamma u + \frac{\partial u}{\partial s^+} - \frac{\partial u}{\partial s^-} = 0 \quad \text{at corners}$$

5.3. PML

Perfectly matched layers (PML) as proposed by Bérenger [5], Bonnet–Poupeau [6] are perhaps the most favoured method these days. In the case of TM polarization, one add to the computational domain an absorbing layer (the coefficient σ) tuned to absorb only in the direction normal to the outer boundary:

$$\begin{aligned} \partial_t H_x + \partial_y E_z + \sigma_2 H_x &= 0 \\ \partial_t H_y - \partial_x E_z + \sigma_1 H_y &= 0 \\ \partial_t E_z - \partial_x H_y + \partial_y H_x + \sigma_1 E_z + (\sigma_2 - \sigma_1) E_z^1 &= 0 \\ \partial_t E_z^2 + \partial_y H_x + \sigma_2 E_z^2 &= 0 \end{aligned}$$

where

$$E_z = E_z^1 + E_z^2, \quad \begin{pmatrix} \sigma_1 \\ \sigma_2 \end{pmatrix} = \frac{18}{\lambda^4} (\vec{x} - \Gamma_\infty)^3$$

See Morgan *et al.* [3] for numerical results for instance.

6. YEE'S SCHEME FOR THE TM MODE

The first and perhaps the best efficient scheme for Maxwell's system discretized by the finite difference method was given by Yee [7].

$$\partial_t E_z = Z \nabla \times \vec{H} \quad \partial_t \vec{H} = \frac{1}{Z} \nabla \times E_x$$

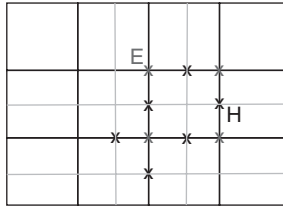


Figure 4. Staggered mesh.

It uses central differences on a staggered grid (Figure 4) and a leap-frog time scheme:

$$E_{z,i,j}^{n+1} = E_{z,i,j}^n - Z \frac{\delta t}{\delta x} (\delta_x H_{y,i,j}^{n+1/2} - \delta_y H_{x,i,j}^{n+1/2})$$

$$H_{x,i,j-1/2}^{n+1/2} = H_{x,i,j-1/2}^{n-1/2} - \frac{\delta t}{Z \delta y} \delta_y E_{z,i,j-1/2}^n$$

$$H_{y,i-1/2,j}^{n+1/2} = H_{y,i-1/2,j}^{n-1/2} + \frac{\delta t}{Z \delta x} \delta_x E_{z,i-1/2,j}^n$$

where δ_x, δ_y are centred difference operators. The scheme is $O(\delta x^2 + \delta t^2)$; 4th order improvement can be found in Reference [8].

7. VALIDATION

To validate a numerical method one can test it against exact solutions. Then one can plot the Sobolev norm error, phase error, diffusion error, etc versus mesh, time step at each time. Typical test problems are the cylinder and the sphere in infinite domain and the rectangle with simple boundary and initial conditions. Visual performance can be acquired by comparing with popular test cases such as the open box problem, the NACA0012 and the CETAF wing.

8. FINITE ELEMENT METHODS

8.1. A conforming method of order 1

Let $Q = (B_x, B_y, D_z)$ then

$$\partial_t Q + \nabla \cdot F(Q) = 0, \quad F = \begin{pmatrix} 0 & \frac{D_z}{\varepsilon} \\ -\frac{D_z}{\varepsilon} & 0 \\ -\frac{B_y}{\mu} & \frac{B_x}{\mu} \end{pmatrix}$$

Morgan *et al.* [3] use *linear elements* plus a 2 step Runge–Kutta time discretization:

$$Q^{n+1/2} = Q^n - \delta t \nabla \cdot F(Q^n) \quad \int_{\Omega} (Q^{n+1} - Q^n)_w = -\delta t \int_{\Omega} w \nabla \cdot F(Q^{n+1/2})$$

on a rectangular shaped domain employing a PML technique. A stability condition is necessary of the CFL type $\delta t \leq ch$. The method requires mass lumping to be explicit but an implicit version with two Jacobi iterations per time step to solve the linear system associated with the mass matrix is sufficient.

8.2. Finite element methods with the Nédélec element

To improve the accuracy on the divergence equations, one may use the Nédélec Element [9] to approximate

$$H(\text{curl}, \Omega) = \{\vec{v} \in L^2(\Omega)^d : \nabla \times \vec{v} \in L^2(\Omega)^d\}$$

Define $d=2$ for two dimensions and $d=3$ for three dimensions. Using

$$V_h = \{\vec{v}_h \in H(\text{curl}, \Omega) : \vec{v}_h|_K \in \mathcal{P}_1^d \quad \forall \text{ triangles } K\}$$

or also

$$V_h = \{\vec{v}_h \in H(\text{curl}, \Omega) : \vec{v}_h = \vec{a}_K + \vec{b}_K \times \vec{x}\}$$

Define τ as the unit tangent vector. The degrees of freedom are the integrals on edges $\int_e (v \cdot \tau)$

Proposition 2

$$\|v - v_h\|_0 + \|\nabla \times (v - v_h)\|_0 < h \|v\|_{1, \text{curl}}$$

where $\|\cdot\|_0$ is the norm of $L^2(\Omega)$ and $\|\cdot\|_{1, \text{curl}}$ the norm of $H(\text{curl}, \Omega)$.

8.3. Stabilization

Elimination of a variable, for instance \vec{E}

$$\mu \partial_t H + \nabla \times \left(\frac{1}{\varepsilon} \nabla \times H \right) = 0$$

plus an implicit centred time scheme gives

$$\begin{aligned} \frac{\mu}{\delta t} H + \nabla \times \frac{1}{\varepsilon} \nabla \times H - \mu \nabla p &= f \\ \nabla \cdot (\mu H) &= g \\ [H \times n] = 0 \quad [\mu H \cdot n] = g \quad [p] = 0, \quad \frac{1}{\varepsilon} [\nabla H \times n] &= f \quad \text{on } \Gamma \\ p = 0, \quad H \times n = 0 &\quad \text{on } \partial\Omega \end{aligned}$$

Note that if $\nabla \cdot f = 1/\delta t g$ then $p=0$.

8.3.1. *Approximation.* Raviart *et al.* [10] used a linear/quadratic conforming element just as for the Stokes problem. Zou *et al.* [11] use the Nedelec element [12, 9] H_h with linear elements for p_h :

$$H_0(\text{curl}) = \{v \in H(\text{curl}) : v \times n = 0 \text{ on } \Gamma\}$$

The variational form is: find $H \in H_0(\text{curl}), p \in H_0^1$ with

$$a(H, B) \equiv \int_{\Omega} \frac{1}{\varepsilon} \nabla \times H \cdot \nabla \times B \quad b(H, q) \equiv - \int_{\Omega} \mu H \cdot \nabla q$$

$$a(H, B) + b(B, p) = \int_{\Omega} f \cdot B - (f \times n, B)_{\Gamma} \quad \forall B \in H_0(\text{curl})$$

$$b(H, q) = \int_{\Omega} g q \quad \forall q \in H_0^1$$

One has existence and uniqueness and for the discrete problem (see Reference [13]) and $O(h)$ because the inf-sup conditions for this mixed problem are satisfied.

9. FINITE VOLUME AND DISCONTINUOUS GALERKIN METHODS

There are two families of finite volume methods, those which use the triangles as their finite volume and those which use the cells formed by the set of triangles which have a common vertex (Figure 5).

Finite Volumes with piecewise constant approximations on cells for $Q = (B_x, B_y, D_z)$ give

$$\partial_t Q + \nabla \cdot F(Q) = 0, \quad F = \begin{pmatrix} 0 & \frac{D_z}{\varepsilon} \\ -\frac{D_z}{\varepsilon} & 0 \\ -\frac{B_y}{\mu} & \frac{B_x}{\mu} \end{pmatrix}$$

Just as for conservation laws in fluid, the finite volume method gives

$$\text{area}(T_k) \partial_t Q_k + \sum_{1,2,3} \bar{F}(Q) n_{ij} = 0$$

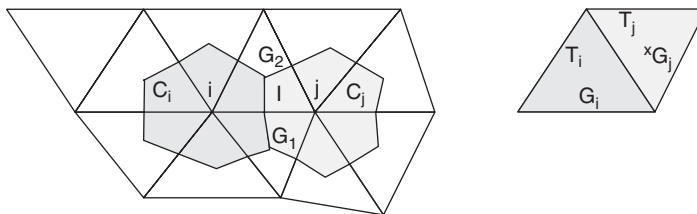


Figure 5. Finite volume cells.

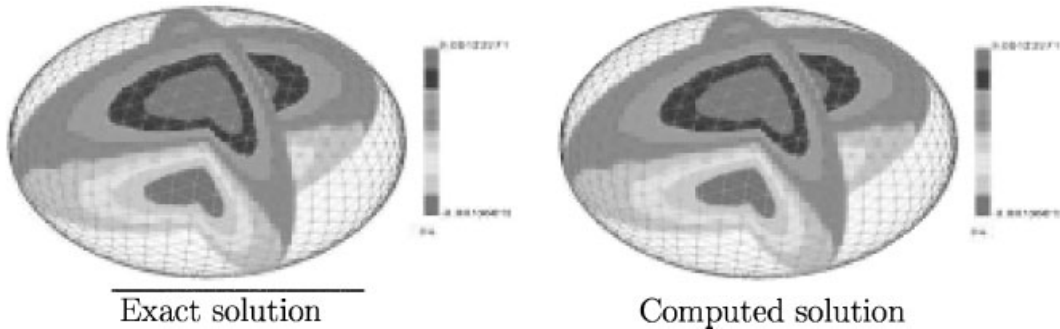


Figure 6. Courtesy of Lala [17].

It can be integrated with the Godunov scheme [14]:

$$A_{ij} = F'(\bar{Q})n_{ij}, \quad \partial_i \bar{Q} + \partial_s(A_{ij}\bar{Q}) = 0, \quad \text{if } n < n_{ij}\bar{Q}(0) = Q_i \text{ else } = Q_j$$

where $\bar{F}(Q) = F(\bar{Q})$.

Second order flux correction and/or discontinuous Galerkin of any degree are also feasible. An implementation by Cioni *et al.* [15] and Remaki [2, 16] is as follows:

- Two step R-K, $CFL < 1/3$ (classical FVM = 0.75, Yee = $1/\sqrt{2}$)
- P^0 with second order correction is about same precision as order 1 yet twice as fast, but somewhat more diffusive.
- Alternatively leap-frog $Q^{n+1} - Q^n = \delta t F(Q^{n+1/2})$ preserves $\mathcal{E} = \frac{1}{2}(\varepsilon E^2 + \mu H^2)$. For $\delta t < ch$ the scheme is L^2 stable. Von Neumann stability condition is $2 \times$ bigger than Yee's ($\delta t < c\delta x$) but equal precision requires a grid $2 \times$ finer (Figure 6).

10. THE EXPLICIT SCHEMES OF BOSSAVIT

Using the theory of tensor calculus, Bossavit [18] proposed to use a leap-frog time stepping scheme with a collocation method based on the use of projection operators from n -forms to m -forms:

$$\frac{B^{n+1/2} - B^{n-1/2}}{\delta t} = \mathcal{A}_h D^n, \quad \frac{D^{n+1} - D^n}{\delta t} = \mathcal{B}_h B^{n+1/2}$$

$$H^{n+1/2} = \frac{1}{\mu} \Pi_h B^{n+1/2}, \quad E^{n+1} = \frac{1}{\varepsilon} \Pi_h D^n$$

E, H and 1-forms are approximated with one degree of freedom per edge while B, D and 2-forms have one degree of freedom per face.

Divergence and Energy are exactly conserved and the scheme is $O(\delta t^2 + h^2)$.

The originality of the scheme is that it treats exactly the PDEs and puts the interpolation operators on the constitutive relations between E and D and H and B . However at best it needs inversion of local mass matrices, requires 7K words of memory per mesh point and is more dispersive than finite volume methods of order 3 yet less diffusive.

It is unconditionally L^2 stable but H^1 stability requires a CFL conditions as usual. It can also be extended to quadrangles (see also Lala [17]).

11. HARMONIC SIGNAL

11.1. Direct methods

If $(E_\infty, H_\infty) = \text{Re}(u_\infty(x), v_\infty(x))e^{i\omega t}$ then after some time

$$\begin{aligned} i\omega\varepsilon E - \nabla \times H &= \hat{J} \\ i\omega\mu H + \nabla \times E &= 0 \\ \nabla \cdot (\mu H) &= \hat{\rho} \\ \nabla \cdot (\varepsilon E) &= 0 \end{aligned}$$

It can be reached by $t \rightarrow \infty$ or least square (Glowinski *et al.* [19]) or augmented with $\partial/\partial t$ or stabilized. The stabilization is as follows (Figure 7):

$$\begin{aligned} i\omega\varepsilon E - \nabla \times H + \nabla p &= \hat{J} \\ i\omega\mu H + \nabla \times E + \nabla q &= 0 \\ \nabla \cdot (\mu H) &= \hat{\rho} \\ \nabla \cdot (\varepsilon E) &= 0 \end{aligned}$$

11.2. TE or TM cases

In the 2d cases (TM or TE) Maxwell's equations reduces to a scalar Helmholtz equation

$$\omega^2 \varepsilon \mu u + \Delta u = 0$$

Any method works but usually produces large ill-conditioned linear system!

11.3. Boundary element method

When ε, μ are constant the following integral equation is equivalent to Maxwell system:

11.3.1. *Electric field integral equation (EFIE)*. For all $\hat{J} // \Gamma$

$$\int_{\Gamma \times \Gamma} \frac{e^{i\kappa|x-y|}}{4\pi|x-y|} [J(y) \cdot \hat{J}(x) - \frac{1}{\kappa^2} \nabla_\Gamma J(y) \cdot \nabla_\Gamma \hat{J}(x)] d\gamma(y) d\gamma(x) = \frac{1}{\kappa Z} \int_\Gamma E^i \cdot \hat{J} d\gamma$$

where γ denotes the elementary area of the surface Γ and Z the impedance.

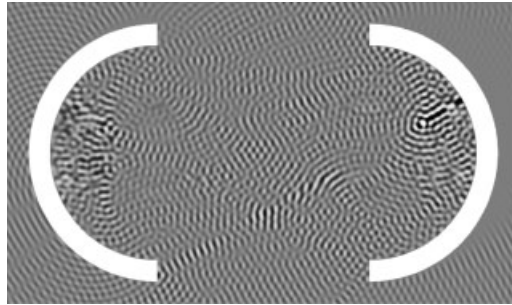


Figure 7. 3D solution of Helmholtz' equation with 1.5 million mesh nodes (from Heikkola [20]).

11.3.2. *Magnetic field integral equation (MFIE)*. Alternatively one may use: for all $\hat{J} // \Gamma$

$$\int_{\Gamma \times \Gamma} \left[\frac{1}{2} J(y) \cdot \hat{J}(x) + \left[n(x) \times \nabla_{\Gamma} \left(\frac{e^{i\kappa|x-y|}}{4\pi|x-y|} \right) \times J(y) \right] \cdot \hat{J}(x) \right] d\gamma(y) d\gamma(x) \\ = \int_{\Gamma} H^i \cdot \hat{J} \times n d\gamma$$

or even combine both to give a more stable equation:

11.3.3. *Combined field integral equation (CFIE)*.

$$\text{CFIE} = \alpha \text{EFIE} + (1 - \alpha) \frac{i}{\kappa} \text{MFIE}$$

where α is a weight factor chosen in $(0,1)$.

11.3.4. *Discretization*. In Schwab [21] the discretization is done with the Raviart Thomas element

$$\mathcal{RT}_0(\Gamma_h) = \{J_h \in H(\text{div}_{\Gamma}, \Gamma) : v_h|_T = \vec{a} + \beta \vec{x}, \quad a_j, \beta \in \mathcal{C}\}$$

for which the degrees of freedom are the edge integrals $\int_e v_h \times n ds$.

Proposition 3

Both the continuous and discrete sesqui-linear forms are the difference of a $H^{-1/2}(\text{div}_{\Gamma}, \Gamma)$ -elliptic sesqui-linear form and a compact sesqui-linear form.

Proposition 4

$$|J - J_h| \leq \inf_{I_h \in G_h} |J - I_h|_G$$

where $G \approx H^{-1/2}(\text{div}_{\Gamma}, \Gamma) \dots$

11.3.5. *Iterative solution.* Consider the Helmholtz equation and let $G(x) = e^{i|x|}/|x|$

$$\Delta u + \kappa^2 u = 0, \quad \partial_n u|_\Gamma = g, \quad r(\partial_n - i\kappa u)|_\infty = 0$$

solved by having $u(x) = \int_\Gamma w(y) \partial_n G(x - y) d\gamma(y)$ for all \hat{w}

$$\int_{\Gamma \times \Gamma} G(x - y) (\nabla w \cdot \nabla \hat{w} - \kappa^2 w \hat{w} n(x) \cdot n(y)) d\gamma(x) d\gamma(y) = \int_\Gamma g \hat{w}$$

discretized by the P^1 element and solved by a conjugate gradient algorithm

$$N_\kappa w = - \int_\Gamma \frac{\partial^2 G}{\partial n(x) \partial n(y)} (x - y) w(y) d\gamma(y)$$

$$S_\kappa w = \int_\Gamma G(x - y) w(y) d\gamma(y)$$

$$D_\kappa w = \int_\Gamma \partial_n G(x - y) w(y) d\gamma(y)$$

Recall the Calderon identity $4S_\sigma N_\kappa = 1 + 4(D_\kappa^2 + (S_\sigma - S_\kappa)N_\kappa)$ shows that $S_\sigma \approx N_\kappa^{-1}$ because the rest is compact.

Proposition 5

$Z = C^{-1} B_\sigma C^{-1}$ is a preconditioner with

$$B_{\sigma ij} = \int_\Gamma w^i S w^j = \int_{\Gamma \times \Gamma} w^i(x) G(x - y) w^j(y) \quad C_{ij} = \int_\Gamma w^i w^j$$

in the sense that $Z^{-1}N$ has condition number $O(1)$ when κ and σ are not near a resonance mode.

11.4. Fast multipole methods

FMM is an acceleration algorithm which makes the overall integral equation solver $O(n \log n)$ where n is the number of discretization points on the surface S . To illustrate the principle of the method we reproduce here the example from Darve [22–24].

For a given large integer J and two given sets of vectors $\{u_j\}_1^J, \{x_j\}_1^J$, let us compute $v_i = \sum_{j=1}^J u_j / (x_i - x_j) \quad i = 1 \dots J$. If no trick is applied it takes J^2 operations. However one may do the following:

$$\frac{1}{x - y} = \frac{1}{x - z + z - y} = \frac{1}{(x - z) \left(1 + \frac{z - y}{x - z}\right)} = \sum_{m=0}^M \frac{(y - z)^m}{(x - z)^{m+1}} + o\left(\left(\frac{z - y}{x - z}\right)^M\right)$$

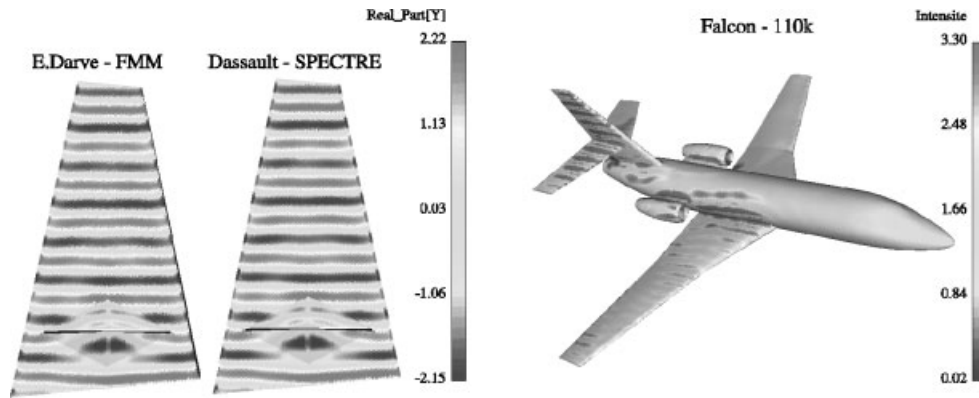


Figure 8. Computations with the FMM (courtesy of E. Darve).

therefore

$$\sum_{j=1}^J \frac{u_j}{x_i - x_j} = \sum_{m=0}^M \left[\sum_{j=1}^J (x_j - z)^m u_j \right] \frac{1}{(x_i - z)^{m+1}} = B_{im} A_{mj} u_j$$

Now the operation count is $2M \times J + M \times M$.

To apply this idea to Maxwell's integral formulation we need special factorized solutions to Maxwell Harmonic equations such as ($\kappa = \omega\sqrt{\epsilon\mu}$)

$$E(x) = \sum_{j \geq 1} \sum_{m \in [-j, j]} \left[u_j^m \frac{h_j(\kappa r)}{h_j(\kappa)} T_j^m(\theta, \varphi) + \frac{i\kappa}{\omega\epsilon} v_j^m \right. \\ \left. \times \left[\frac{j+1}{2j+1} \frac{h_{j-1}(\kappa r)}{h_j(\kappa)} I_{j-1}(\theta, \varphi) + \frac{j}{2j+1} \frac{h_{j+1}(\kappa r)}{h_j(\kappa)} N_{j+1}^m(\theta, \varphi) \right] \right]$$

Rokhlin [25], Greengard [26], Chew [27], Darve [22] have perfected the method. Here are some results (Figure 8).

12. CONCLUSION

There are 3 families of methods: time methods, frequency FEM methods, BEM-FMM. FMM is fastest but difficult for non-constant materials. Direct time formulation is most general and can handle any radar pulse but may be slow to converge. Frequency methods are a good compromise at present. However more research on preconditioners is needed. More generally authors unfortunately do not pay attention to the standardization of test cases and this makes the comparisons difficult. To allow finite difference methods to be general one needs to use the fictitious domain embedding method. For inverse scattering the handling of thin

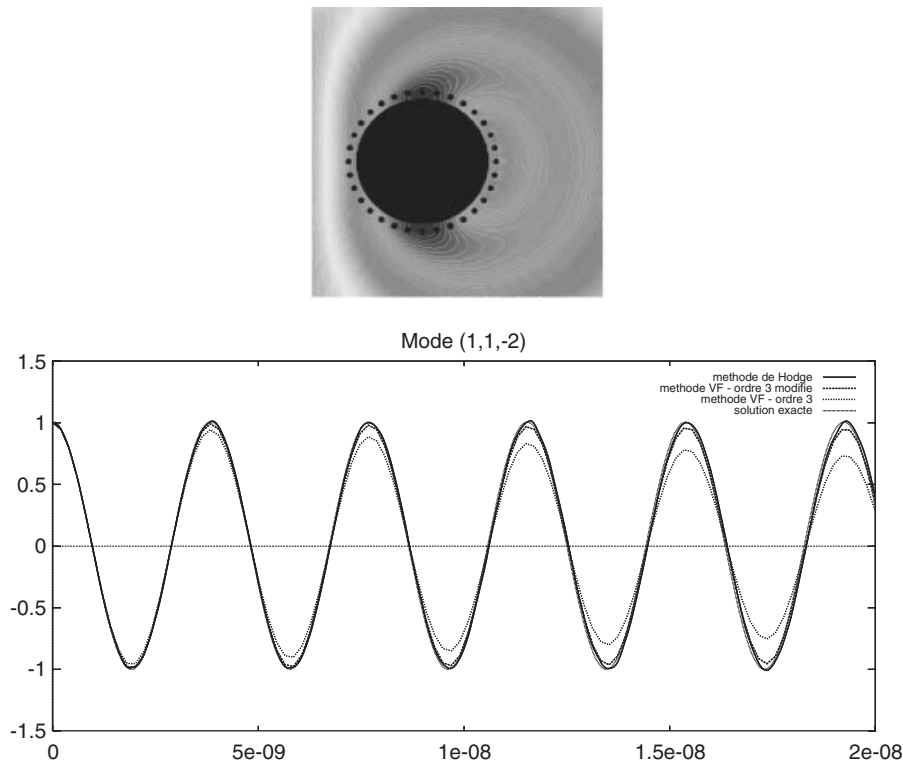


Figure 9. Comparison with a finite volume method on the same mesh (courtesy of Remaki [2]).

layers of composite materials are essential but we have not covered this aspect in this report (Figure 9).

REFERENCES

1. Skolnik MI. *Introduction to Radar Systems*. McGraw-Hill: New York, 1980.
2. Remaki M, Loula Fézoui. Une méthode de Galerkin Discontinuu pour la résolution des équations de Maxwell en milieu hétérogène. *INRIA Report No. 3501*, September 1998.
3. Morgan K, Hassan O. Pegg NE, Weatherill NP. The simulation of electromagnetic scattering in piecewise homogeneous media using unstructured grids. *Computational Mechanics* 2000; **25**:438–447.
4. Grote MJ, Keller JB. Nonreflecting boundary conditions for Maxwell's equations. *Journal of Computational Physics* 1998; **139**(2):327–343.
5. Béranger, JP. Three-dimensional perfectly matched layer for the absorption of electro-magnetic waves. *Journal of Computational Physics* 1996; **127**:363–379.
6. Bonnet F, Poupaud F. Béranger's absorbing boundary conditions with time volume scheme for triangular meshes. *Applied Numerical Mathematics* 1995; **25**:333–354.
7. Yee KS. Numerical solution of initial boundary value problems involving Maxwell's equations in isotropic media. *IEEE Transactions on Antennas and Propagation* 1966; **14**:302–307.
8. Yefet A, Petropoulos P. A non-dissipative staggered fourth order accurate explicite FDM scheme. *ICASE Report* 99-30, 1998.
9. Nédélec J-C. A new family of mixed finite elements in \mathbb{R}^3 . *Numerical Mathematics* 1986; **50**:57–81.
10. Raviart PA. Finite element approximation of the time-dependent Maxwell equations. *Technical Report GdR SPARCH*, vol 6. Ecole Polytechnique, France, 1993.

11. Ciarlet P Jr, Zou J. Finite element convergence for the Darwin model to Maxwell's equations. *RAIRO Mathematical Modelling in Numerical Analysis* 1997; **31**:213–250.
12. Ciarlet P-G. *The Finite Element Method*. Prentice-Hall: Englewood Cliffs, NJ, 1977.
13. Monk P, Demkowicz L. Discrete compactness and the approximation of Maxwell's equations in \mathcal{R}^3 . *Mathematics of Computing* 2001; **70**(234):507–523.
14. Godunov SK. A finite difference method for the computation of discontinuous solutions of the equations of fluid dynamics. *Siberian Journal of Mathematics* 1959; **47**:271–290.
15. Cioni JP, Remaki M. Comparaison de deux méthodes de volumes nis en électromagnétisme. *Rapport de recherche INRIA* No 3166, Mai 1997.
16. Remaki M. A new finite volume scheme for solving Maxwell's system. *COMPEL—The International Journal for Computation and Mathematics in Electric and Electronic Engineering* 2000; **19**(3):913–931.
17. Lala S, de La Bourdonnaye A. A finite element method for Maxwell system preserving Gauss laws and energy. *INRIA Report No.* 3557, Nov 1998.
18. Bossavit A. Un nouveau point de vue sur les éléments mixtes. *MATAPLI* 1989; **20**:23–35.
19. Glowinski R, Pan TW, Periaux J. A fictitious domain method for external incompressible viscous flow modeled by Navier–Stokes equations. *Computer Methods in Applied Mechanics and Engineering* 1994; 283–303.
20. Heikkola E, Rossi T, Toivanen J. A parallel fictitious domain method for the 3D Helmholtz equation. *Proceedings of the 9th SIAM Conference on Parallel Computing*. SIAM: Philadelphia, PA, 1999.
21. Hiptmair R, Schwab C. Natural BEM for the Electric Field Integral Equation on polyhedra. Preprint EPFL, 2001.
22. Darve E. Fast multipoles: a mathematical study (abridged version). *Comptes Rendus des Seances de l'Academie des Sciences. Serie I. Mathematique* 1997; (t. **325**):1037–1042.
23. Darve E. The fast multipole method: numerical implementation. *Journal of Computational Physics* 2000; **160**(1):195–240.
24. Darve E. Méthodes multipôles rapides: résolution des équations de Maxwell par formulations intégrales. *Ph.D.* in Applied Math, Université Pierre et Marie Curie, Paris, June 1999.
25. Rokhlin V. Diagonal forms of translation operators for the Helmholtz equation in three dimensions. *Research Report YALEU/DCS/RR-894*, Yale University Department of Computer Science, March 1992.
26. Greengard L, Huang J. A new version of the fast multipole method for screened Coulomb interactions in three dimensions. *Journal of Computational Physics* 2002; **180**(2):642–658.
27. Chew WC. Fast algorithms for wave scattering developed at the University of Illinois electromagnetics laboratory. *IEEE Antennas Propagation Magazine* 1993; **35**(4):22–32.
28. Assous F, Degond P, Heintzé E, Raviart P-A, Segré J. On a finite element method for solving the three-dimensional Maxwell equations. *Journal of Computational Physics* 1993; **109**:222–237.
29. Cessenat M. *Mathematical Methods in Electromagnetism*. World Scientific: River Edge, NJ, 1998.
30. Christiansen SH, Nédélec J-C. Des préconditionneurs pour la résolution numérique des équations intégrales de frontière de l'acoustique *Comptes Rendus des Seances de l'Academie des Sciences. Serie I. Mathematique* 2000; **330**:617–622.
31. Greengard L. Fast algorithms for classical physics. *Science* 1994; **265**(5174):909–914.
32. Monk P. Analysis of finite element method for Maxwell's equations. *SIAM Journal on Numerical Analysis* 1992; **29**:714–729.
33. Nicolaidis R, Wang D-Q. Convergence analysis of covolume scheme for Maxwell's equations in three dimensions. *Mathematics of Computing* 1998; **67**:947–963.
34. Petitjean B, Löhner R. Finite element solvers for radar cross section RCS calculations. *AIAA Paper* 92-0455, 1992.
35. Poupaud F, Remaki M. Existence and uniqueness of the maxwell's system solutions in heterogeneous and irregular media. *Comptes Rendus des Seances de l'Academie des Sciences. Serie I. Mathematique* 2000; **330**:99–103.
36. Rokhlin V. Rapid solution of integral equations of scattering theory in two dimensions. *Journal of Computational Physics* 1990; **86**(2):414–439.